Preprint Title	One-Pot Synthesis of Oxazolidinones and Five-Membered Cyclic Carbonates from Epoxides and Chlorosulfonyl isocyanate: Theoretical Evidence for the Asynchronous Concerted Pathway
Authors	Esra Demir, Özlem Sarı, Yasin Çetinkaya, Ufuk Atmaca, Safiye Sağ Erdem and Murat Celik
Publication Date	14 Apr 2020
Article Type	Full Research Paper
Supporting Information File 1	Supporting Information.doc; 5.2 MB
ORCID® iDs	Ufuk Atmaca - https://orcid.org/0000-0002-5598-0443; Murat Celik - https://orcid.org/0000-0003-3485-7822

One-Pot Synthesis of Oxazolidinones and Five-Membered Cyclic Carbonates from Epoxides and Chlorosulfonyl isocyanate: Theoretical Evidence for the Asynchronous Concerted Pathway

Esra Demir[1], Ozlem Sari[2], Yasin Çetinkaya[3], Ufuk Atmaca[1,3], Safiye Sağ Erdem[4], Murat Çelik[*1]

[1]Department of Chemistry, Faculty of Science, Atatürk University, 25240 Erzurum, Turkey
[2]Department of Chemistry, Faculty of Arts and Sciences, Kırşehir Ahi Evran University, 40100 Kırşehir, Turkey
[3]Department of Food Technology, Oltu Vocational School, Atatürk University, 25400 Oltu, Erzurum, Turkey
[4]Department of Chemistry, Faculty of Arts and Sciences, Marmara University, Goztepe Campus, 34722 Istanbul, Turkey

Abstract: The one-pot reaction of chlorosulfonyl isocyanate (CSI) with epoxides having substituted phenyl, benzyl and fused cyclic alkyl groups in different solvents under mild reaction conditions without additives and catalysts was studied. Oxazolidinones and five-membered cyclic carbonates were obtained with a ratio close to (1:1) in the cyclization reactions. The best reaction conversion for the synthesis of these compounds was carried out in dichloromethane (DCM). The method presented here has distinct advantageous over the existing methods such as one-pot reaction, shorter reaction times, metal-free reagent, good yields and very simple purification method. The mechanism for the cycloaddition reactions has been elucidated using density functional theory (DFT) method at the M06-2X/6-31+G(d,p) level. The investigation of the potential energy surfaces associated with two possible channels leading to oxazolidinones and five-membered cyclic carbonates revealed that the cycloaddition reaction takes place through an asynchronous concerted mechanism in gas phase and in DCM.

Keywords: Oxazolidinone; 1,3-Dioxolan-2-ones; Chlorosulfonyl isocyanate; Computational modeling; Density Functional Theory

Introduction

Oxazolidinones (**1**), five-membered heterocyclic rings containing nitrogen atom and ester group, are important compounds in organic chemistry and pharmaceutical chemistry because of their considerable interest as antibiotics [1], immunomodulatories [2], antibacterials [3], as well as synthetic intermediates and chiral auxiliaries for various organic conversions [4-7].

Linezolid [1-3] (**3**) and cytoxazone [8,9] (**4**) are oxazolidinone derivatives having significant biological activities. Linezolid (**3**) approved as a drug in 2000 by the Food and Drug Administration (FDA) is the first and only oxazolidinone drug for the treatment of multidrug resistant Grampositive bacterial infections including methicillin resistant Staphylococcus aureus (MRSA), penicillin resistant Streptococcus pneumoniae (PRSP) and vancomycin resistant Enterococcus faecalis (VRE) (Scheme 1) [10]. Tedizolid phosphate (trade name Sivextro) is another oxazolidinone-class antibiotic being more potent against enterococci and staphylococci when compared with Linezolid [11]. Befloxatone and Toloxatone containing oxazolidinone rings are reversible inhibitors of monoamine oxidase (MAO) [12,13]. N-aryl-oxazolidinedione compounds, which are toloxatone derivatives, have been reported to exhibit good affinity for hMAO-A [14].

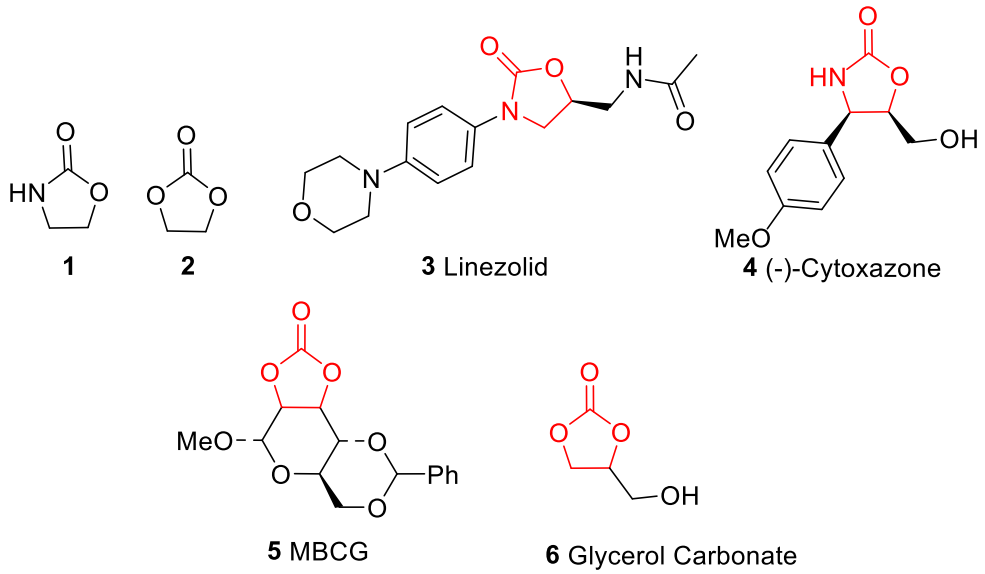

Scheme 1. Oxazolidinone (**1**), five-membered cyclic carbonates (**2**) and some important compounds containing oxazolidinone ring (**3**, **4**) and five-membered cyclic carbonates (**5**, **6**).

Five-membered cyclic carbonates (1,3-dioxolan-2-ones) (**2**) are valuable synthetic targets on account of several applications and pertinent properties. They are found in various natural and potential pharmaceutical products [15]. Moreover, they are used as electrolyte components in Li-ion re-chargeable cells and as aprotic polar solvent with high boiling point as alternative of dangerous solvents because of their good biodegradability and low toxicity [16-18]. Synthetic intermediates for ring-opening polymerization of the compounds containing cyclic carbonates such as methyl 4,6-*O*-benzylidene-2,3-*O*-carbonyl-α-D-glucopyranoside (MBCG) (**5**) [19-20] and glycerol carbonate (**6)** [21] were also reported (Figure 1).

Therefore, numerous synthetic approaches have been developed to date for the preparation of oxazolidinones and five-membered cyclic carbonates in various structures. The most well-known strategies for the synthesis of oxazolidinones are the reaction of an amino alcohol with phosgene [5,22], carbonylation reaction of *β*-amino alcohols with CO_2 or dialkyl carbonates [23-27], multicomponent reaction by rare-earth metal amides [28], reaction of CO_2 with propargylamines or aziridines [29,30] and cycloaddition reaction of epoxides with isocyanates [31,32]. On the other hand, for synthesis of five membered cyclic carbonates, the cycloaddition of CO_2 to epoxides, the reaction with the metal complexes or catalysts, and the reaction of a diol with toxic phosgene are the most common processes [16,17,33-36].

CSI, an highly reactive and versatile isocyanate, reacts with epoxides to give five-membered cyclic carbonates and oxazolidinones [37-39]. In 1984, Keshava Murthy and Dhar reported the synthesis of five-membered cyclic carbonates and oxazolidinones from various epoxides in two steps using CSI and KOH in benzene:dichloromethane (5:1) [40,41]. Five membered cyclic carbonates were formed as the main product in the reaction mixture. It is also known today that benzene is carcinogenic, and not preferred as a solvent unless it is necessary. In 1986, De Meijere and coworkers reported the cyclic addition of CSI to epoxides at -78 ^{o}C to give five membered cyclic carbonates and oxazolidinones [42]. They reported seven reactions; three of these attempts resulted in five membered cyclic carbonates as the sole product while two cases produced oxazolidinones, and other two reactions gave the mixture of two products. These reports prompted us to explore this reaction in more detail. In our previous studies, we investigated the reactions of various carboxylic acids, alkenes and allyl or benzyl alcohols with CSI [43-46]. As a continuation of these studies, we performed one-pot synthesis of the titled compounds by optimizing the reaction of CSI with epoxides in different solvents under mild conditions. Compared to the De Meijere and coworkers's method, the study provided higher yields using simple purification method in shorter reaction times under the mild reaction conditions.

Keshava Murthy and Dhar [41] postulated a mechanism proceeding via a zwitterionic intermediate. C-O bond cleavage from this unstable and strained intermediate gives rise to a short-lived carbonium ion which will attacked by nucleophilic part of the zwitterion in a

concerted way (Scheme 2a). De Meijere and coworkers [42] proposed a mechanism involving a 1,5-dipolar intermediate (Scheme 2b).

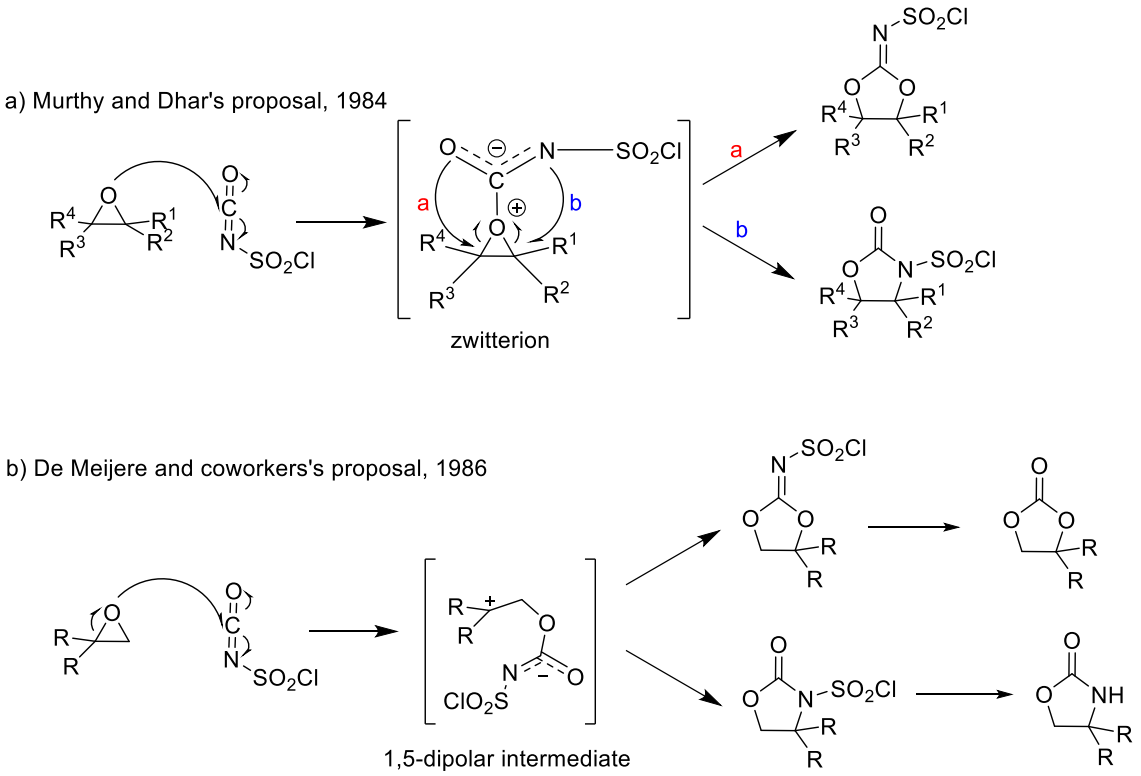

Scheme 2. Proposed mechanisms by Murthy, Dhar [41] and De Meijere and coworkers [42].

To the best of our knowledge, there is no computational mechanistic study in the literature regarding the reaction of epoxides with CSI. On the other hand, the reaction of isocyanates with monofluoroalkenes and nitrones were modeled by quantum chemical calculations [34,47]. Shellhamer et al. [37] explored the reaction mechanism of monofluoroalkenes with CSI using Møller-Plesset (MP2) perturbation theory (Scheme 3). Their results showed that the concerted mechanism is preferred over the stepwise pathway.

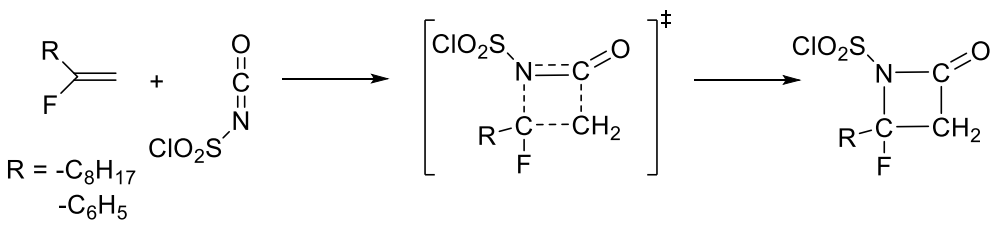

Scheme 3. Reaction of monofluoroalkenes with CSI.

Darù et al. [47] applied DFT calculations using M06-2X functional to investigate the reaction mechanism of cycloaddition reaction of nitrones with isocyanates (Scheme 4). According to their proposal, the mechanism proceeds through a concerted mechanism in gas phase or in nonpolar solvents (hexane and toluene) but a stepwise mechanism in polar (acetonitrile) and moderately polar (dichloromethane and chloroform) solvents.

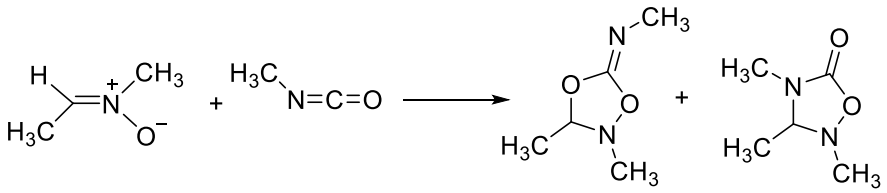

Scheme 4. Cycloaddition reactions of nitrones with isocyanates.

Because the mechanisms of the similar reactions are not completely understood, this inspired us to carry out quantum chemical calculations to enlighten the reaction mechanism for the formation of oxazolidinone and five-membered cyclic carbonates.

Results and discussion:

First, we synthesized various epoxides (**7a-j**) in the presence of *meta*-chloroperbenzoic acid, (*m*-CPBA) from the corresponding alkenes dissolved in DCM at room temperature. The detailed experimental conditions for conversion of alkenes to related epoxides were given in supplementary information. For the synthesis of oxazolidinones and five-membered cyclic carbonates, first the most effective solvent was determined based on the reaction of 8-oxabicyclo [5.1.0] octane (**7b**) with CSI (Table 1). The reaction was carried out in acetone, THF, acetonitrile, dichloromethane, toluene, and *n*-hexane:dichloromethane. While no reaction was observed in diethylether, the best conversion was achieved in dichloromethane. Benzene was not used as a solvent because of having toxic and carcinogenic effects.

Table 1. Solvent optimization for the synthesis of five-membered cyclic carbonates **8b** and oxazolidinone **9b** from epoxide **7b** having substituted fused cyclic alkyl.

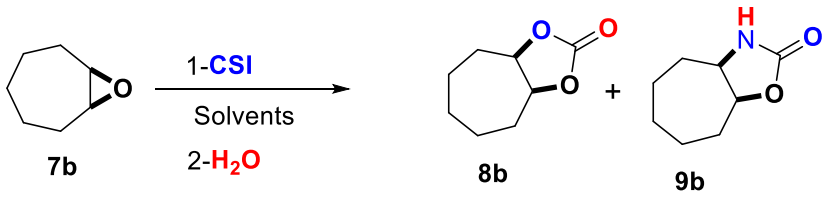

Entry	Solvents	Products (%)[a]	
		Five-membered cyclic carbonate **8b**	Oxazolidinone **9b**
1	Acetone	11	15
2	THF	15	12
3	Diethylether	No reaction	
4	CH_3CN	39	34
5	**Dichloromethane**	**48**	**45**
6	Toluene	13	15
7	n-Hexane: Dichloromethane (1:1)	21	19

[a] Isolated yield.

Herein, we report mild reaction conditions for one-pot synthesis of oxazolidinones and five-membered cyclic carbonates from various epoxides (**7a-j**) at room temperature without using any catalyst.

Table 2. Direct conversion into five-membered cyclic carbonates **8a-j** and oxazolidinones **9a-j** from epoxides **7a-j** by CSI.

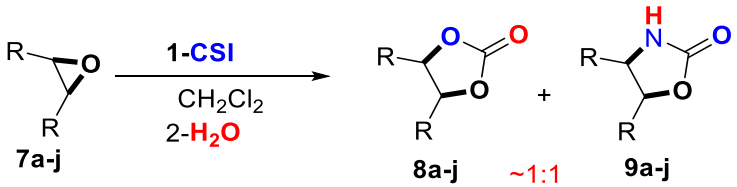

Entry	Substrates	Products[a] (%)	
		Five-membered cyclic carbonates[b]	Oxazolidinones[b]
1	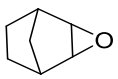 **7a**	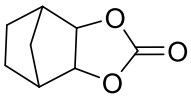 42% **8a** [48]	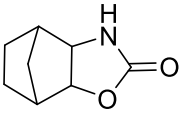 38% **9a** [49]
2	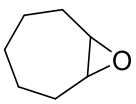 **7b**	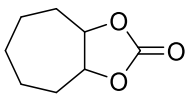 48% **8b** [50]	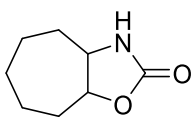 45% **9b** [51]

3	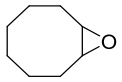 **7c**	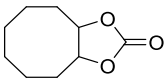 51% **8c** [50]	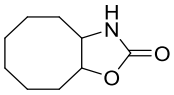 40% **9c**
4	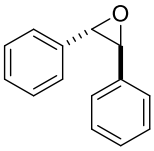 **7d**	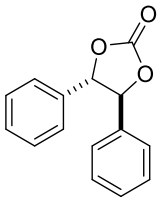 43% **8d** [50]	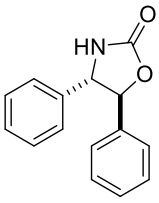 34% **9d** [52]
5	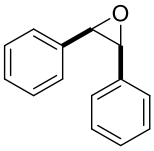 **7e**	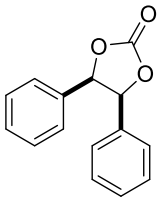 44% **8e** [50]	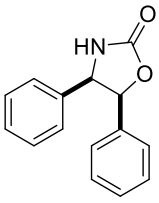 41% **9e** [52]
6	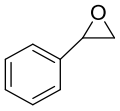 **7f**	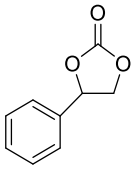 49% **8f** [16]	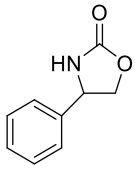 42% **9f** [16]
7	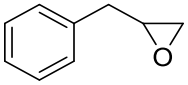 **7g**	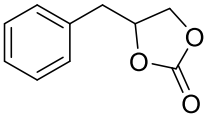 41% **8g** [16]	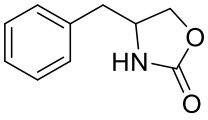 35% **9g** [53]
8	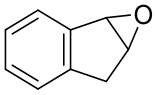 **7h**	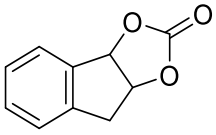 45% **8h** [54]	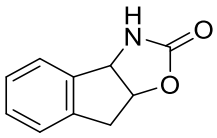 40% **9h** [52]
9	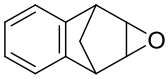 **7i**	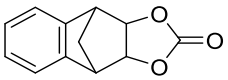 43% **8i**	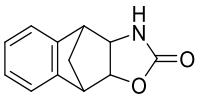 37% **9i**
10	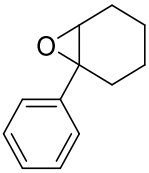 **7j**	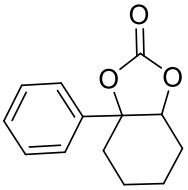 44% **8j**	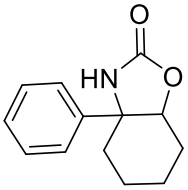 42% **9j** [52]

[a] Isolated yield. [b] Literature.

After having obtained the optimal conditions for the reaction observed, we examined the reactivity of various epoxides to standardize the reaction. Using the optimized conditions, chlorosulfonyl isocyanate was treated with simple epoxides. This approach will allow us to reach different cyclic carbonates and oxazolidinones with a ratio close to (1:1) as shown in Table 2. Trans stilbene (**7d)** and cis stilbene **(7e)** in the presence of CSI gave trans 4,5-diphenyl-1,3-dioxolan-2-one (**8d**), trans 4,5-diphenyloxazolidin-2-one (**9d**) and cis 4,5-diphenyl-1,3-dioxolan-2-one (**8e**), cis 4,5-diphenyloxazolidin-2-one (**9e**), respectively (Table 2). These results show that stereoselectivity is preserved. 4-Phenyl-1,3-dioxolan-2-one (**8f**) and 4-phenyloxazolidin-2-one (**9f**) were obtained from the reaction of CSI with styrene oxide (**7f)** showing the regioselective nature of the reaction. Herein, we report the synthesis of novel oxazolidinone derivatives **8i**, **8j** and 1,3-dioxolan-2-ones **9c** and **9i.** Furthermore, an efficient and straightforward method for the formation of **8a-h**, **9a-b**, **9d-h** and **9j** was described. This synthetic strategy represents a reasonable methodology for the conversion of epoxides to protected 1,2-diols and 1,2-amino alcohols.

Computational results:

A detailed mechanistic investigation of the synthesis of oxazolidinone and five-membered cyclic carbonate derivatives by the reaction between epoxide **7f** and CSI has been performed.

Formation of oxazolidinone 9f: There are two possible channels for the cyclization reaction of epoxide **7f** with CSI to form oxazolidinone intermediates **10** and **11** as shown in Scheme 5. In both transition states it is found that ring-opening reaction of epoxide, nucleophilic attack of N4 onto C1 or C2 and attack of O3 on C5 occur in an asynchronous concerted manner. The first transition state (**TS1**) corresponds to the nucleophilic attack of N4 onto the C2 of **7f** leading oxazolidinone intermediate **10**. The alternative transition state (**TS1′**) corresponds to nucleophilic attack of N4 onto less hindered C1 atom of the epoxide **7f** forming intermediate **11**. Optimized geometries of transition structures are depicted in Figure 1.

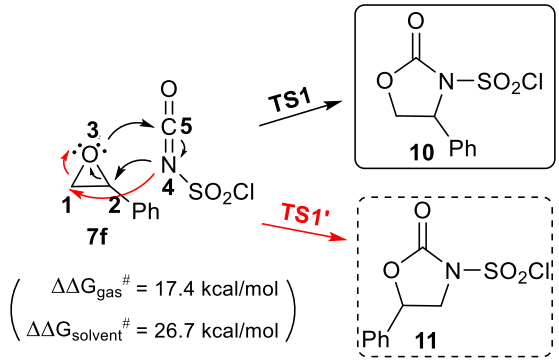

Scheme 5. Possible pathways for the formation of oxazolidinone intermediates **10** and **11**.

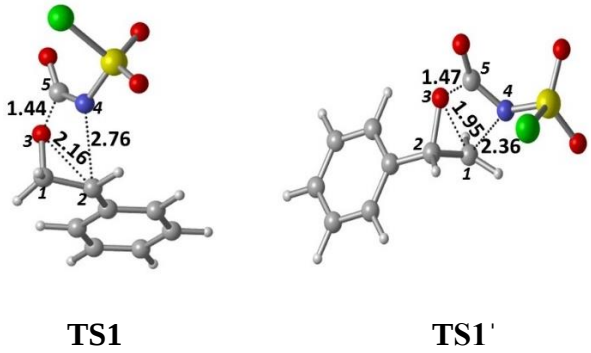

Figure 1. Two possible transition structures for the reaction of **7f** with CSI at PCM/M06-2X/6-31+G(d,p)//M06-2X/6-31+G(d,p) level in DCM. Distances are given in Å.

Our calculated results for the reaction indicate 17.4 kcal/mol (gas phase) and 26.8 kcal/mol (in DCM) preference for the **TS1** over the **TS1′** (Figure 2). Therefore, attack by N4 of CSI on the C2 of epoxide is found to be energetically the most favored approach.

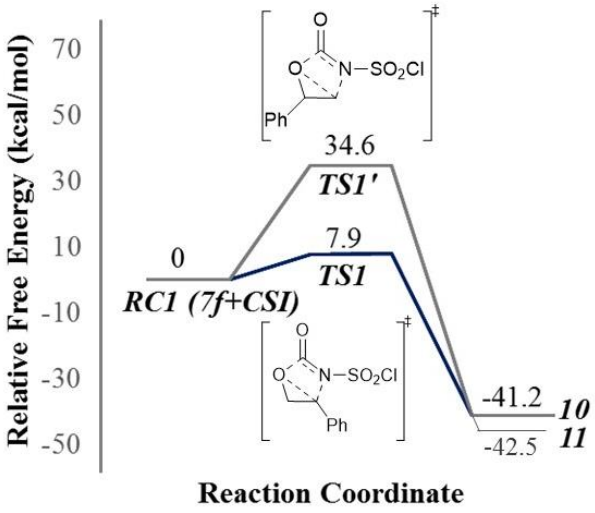

Figure 2. Potential energy profile related to the formation of oxazolidinone intermediates **10** and **11** at the PCM/M06-2X/6-31+G(d,p)//M06-2X/6-31+G(d,p) level in DCM. (Polarization effect of the solvent was considered implicitly.)

Epoxide ring opening and formation of O−C(=O) bond are almost completed before C−N bond is formed. The changes in bond lengths along the intrinsic reaction coordinate (IRC) are depicted in Figure 3a,b as an acceptable approach in the literature [56]. For the formation of **10**, O−C(=O) distance is shortened and C2−O3 bond is elongated rapidly until reaching the product, while the C2−N4 distance is shortened from 2.76 A° in **TS1** to 2.59 A° in **I-41** (Figure 3a). Note that **I-41** is not yet the product but the 41st point in IRC where the C2-N4 distance will eventually decrease to the bond distance when the number of IRC points are increased. These results refer asynchronous events. Same trend is observed for the formation of **11** as shown in Figure 3b. Noteworthy, C2−N4 bond length does not change much along the IRC for the formation of **10**; however, it is shortened more rapidly to give **11**. The presence of partial double bond between C2−C(Ph) (benzylic position) allows electron delocalization around the reacting center, which results in stabilization of transition state and so lowering the activation energy barrier (Figure 3a). On the other hand, stabilization of the benzylic cation is not possible along the IRC path for **TS1′** (Figure 3b), since the bond distance C2−C(Ph) is found as around 1.50 Å showing a single bond character. This can be the main reason for the predominant formation of intermediate **10** which results in the regioselective formation of oxazolidinone **9f**.

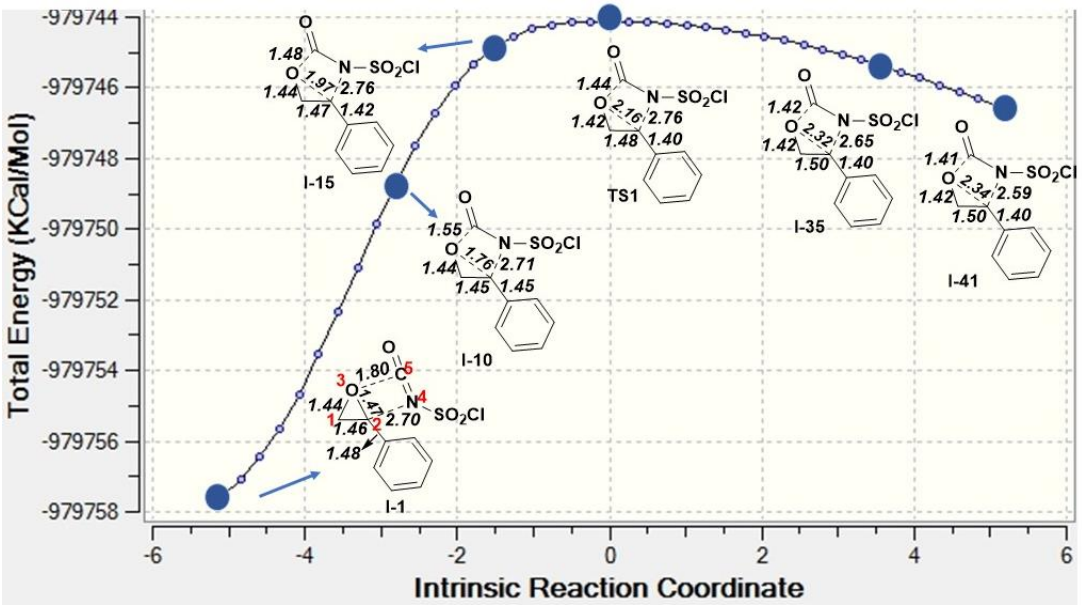

(a)

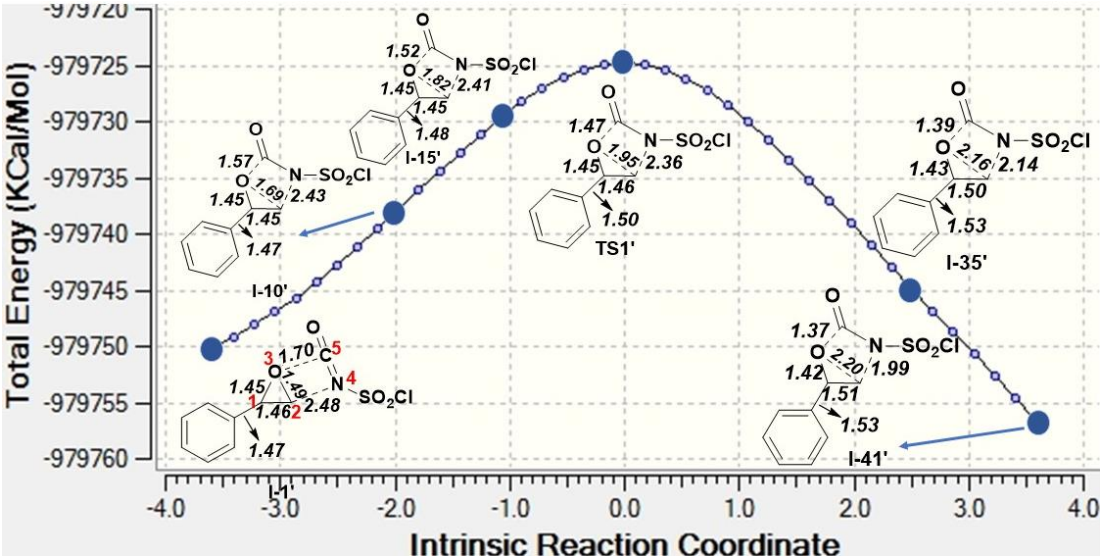

(b)

Figure 3. IRC calculated for the formation of (a) **10** and (b) **11** at M06-2X/6-31+G(d,p) level. **I-1**, **I-15**, **I-35**, **I-41**, etc. are the selected points along the coordinate. Distances are given in Å.

Optimized geometries for reactant complex **RC1 (7f+CSI)**, transition state **TS1** and **10** for the selected path are depicted in Figure 4. This step is common for all paths studied which will be described below.

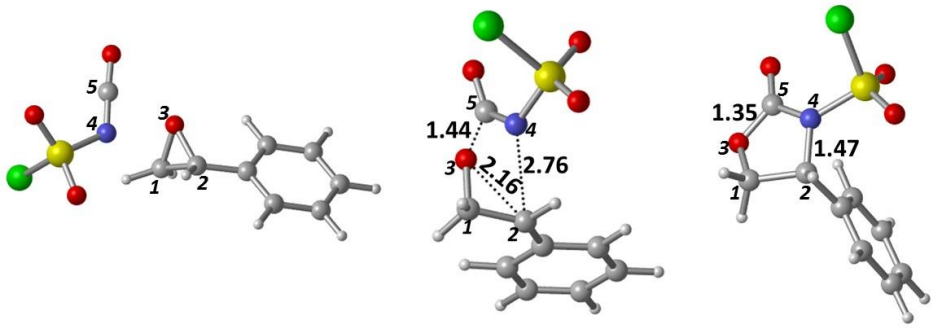

RC1 (7f+CSI) **TS1** **10**

Figure 4. Optimized geometries for the stationary points for the formation of **10** at PCM(DCM)/M06-2X/6-31+G(d,p)//M06-2X/6-31+G(d,p) level (common step of Path 1a, Path 1b and Path 2). Distances are given in Å.

Once **10** is formed, the next step is addition of water. Water addition step can occur via three different pathways namely path 1a, path 1b and path 2 as shown in Scheme 6. The potential energy profile of each path was generated relative to the energy of the initial reactant complex **RC1 (7f+CSI)** (Figure 5). Paths 1a and 1b represent the protonation of ring nitrogen via one and two water molecules, respectively and the departure of **12**. In path 1a, the transformation

of the **TS2** to **9f** involves the shortening of the N4–H8 distance from 1.46 to 1.01 Å and S6–O7 distance from 1.89 to 1.54 Å. This path occurs via four-membered ring transition state **TS2** with an energy barrier of 24.3 kcal/mol relative to **RC1 (7f+CSI)** (Figure 6).

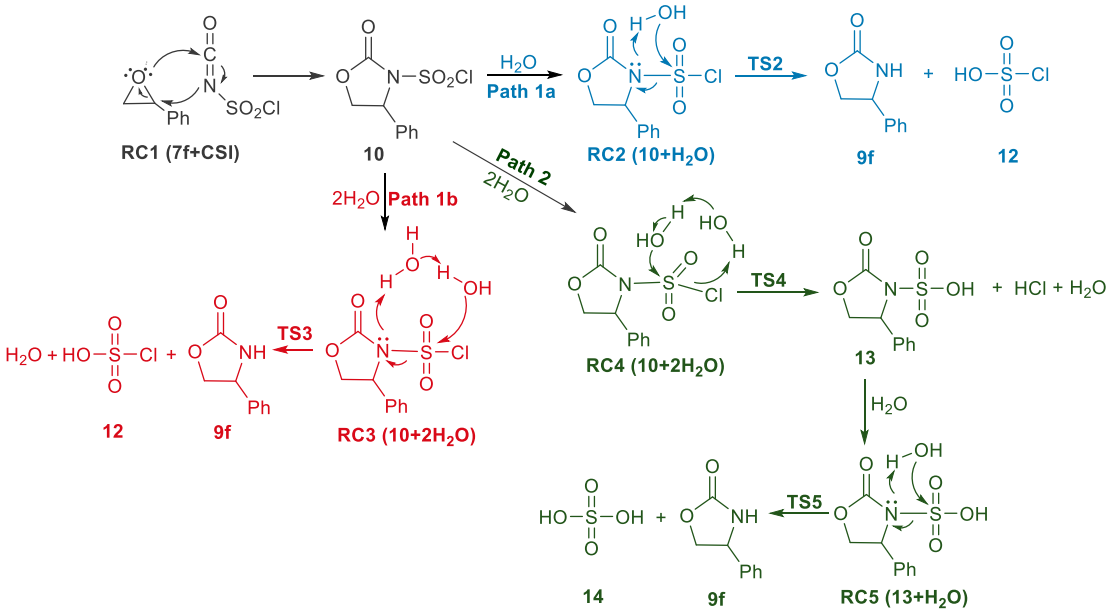

Scheme 6. Proposed mechanism for the formation of oxazolidinone **9f**.

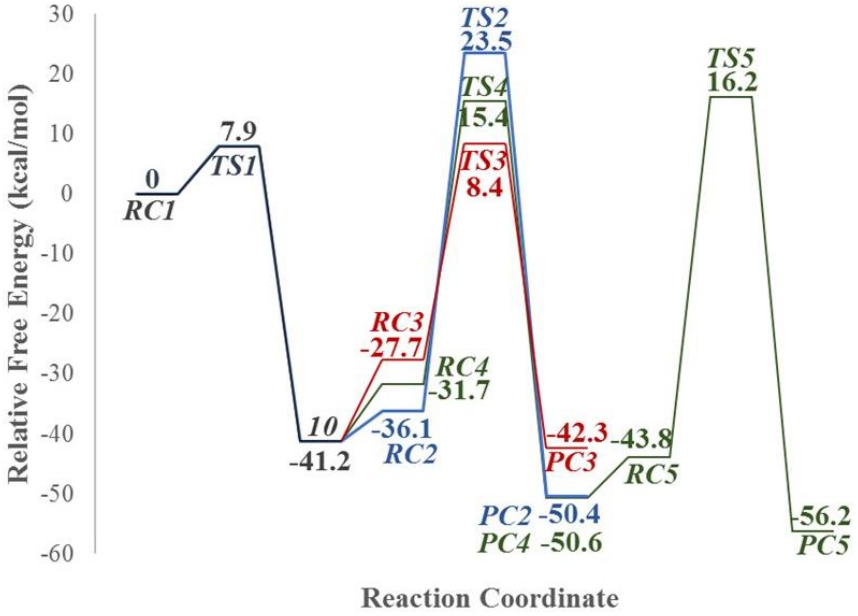

Figure 5. Potential energy profile and relative Gibbs free energies (kcal/mol) in DCM related to the formation of **9f** at PCM(DCM)/M06-2X/6-31+G(d,p)//M06-2X/6-31+G(d,p) level.

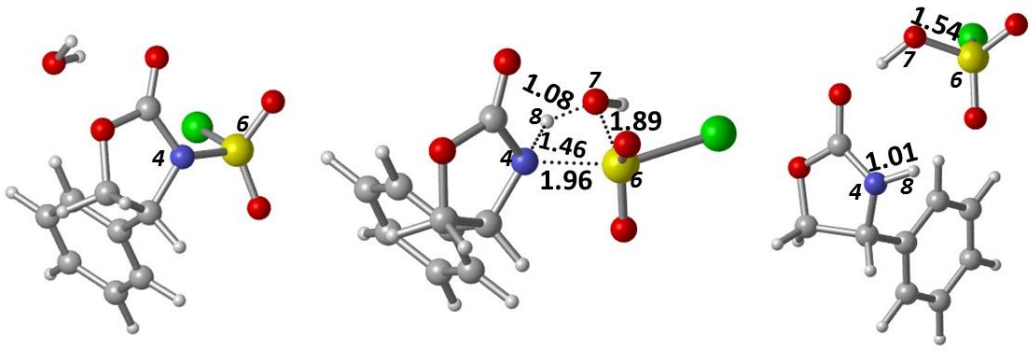

RC2 (10+H_2O) **TS2** **PC2 (9f+12)**

Figure 6. Optimized geometries for the stationary points of path 1a at PCM(DCM)/M06-2X/6-31+G(d,p)//M06-2X/6-31+G(d,p) level. Distances are given in Å.

Other scenario (path 1b) is the direct participation of two water molecules in six-membered **TS3** leading to the target product **9f**. As can be seen from Figure 7, the distance of N4−H8 is calculated as 1.41 Å in **TS3**, which is further shortened to 1.06 Å in **PC3 (9f+12+H_2O)**. Obviously, the proton shuttle activation mechanism pathway is energetically more favorable, which involves a lower barrier of 8.4 kcal/mol with respect to **RC1 (7f+CSI)** (Figure 5).

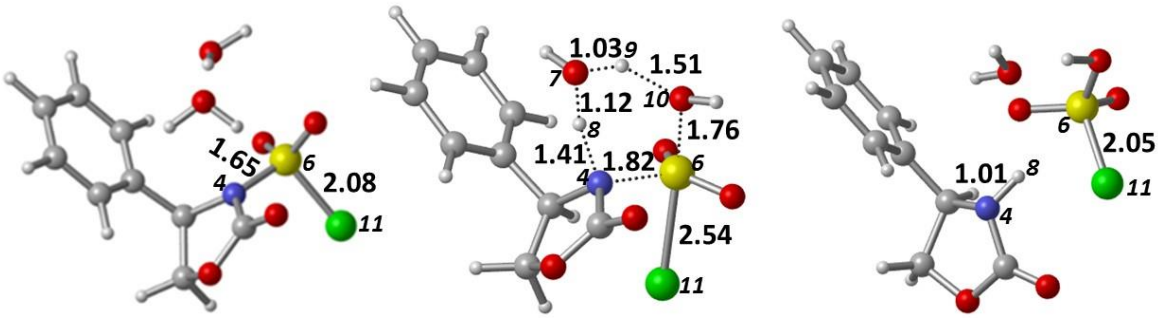

RC3 (9f+2H_2O) **TS3** **PC3 (9f+12+H_2O)**

Figure 7. Optimized geometries for the stationary points of path 1b at PCM(DCM)/M06-2X/6-31+G(d,p)//M06-2X/6-31+G(d,p) level. Distances are given in Å.

Alternatively, the mechanism may proceed through path 2 where the addition of water molecules to the chlorosulfonyl moiety and the departure of H_2SO_4 are observed (Scheme 6). The first step of path 2 involves addition of two water molecules to **RC4 (10+2H_2O)** resulting in elimination of hydrated HCl and formation of **13**. The calculated free energy of activation was found to be 15.4 kcal/mol with respect to **RC1 (7f+CSI)** (Figure 5). Final step of path 2 takes place from **RC5 (13+H_2O)** passing through **TS5** and forming the target product **9f**. This

step requires an activation free energy of 16.2 kcal/mol with respect to initial reactant complex **RC1 (7f+CSI)** (Figure 5). The overall process is exothermic by 56.2 kcal/ mol. Three-dimensional (3-D) views of all the optimized structures of path 2 are illustrated in Figure 8.

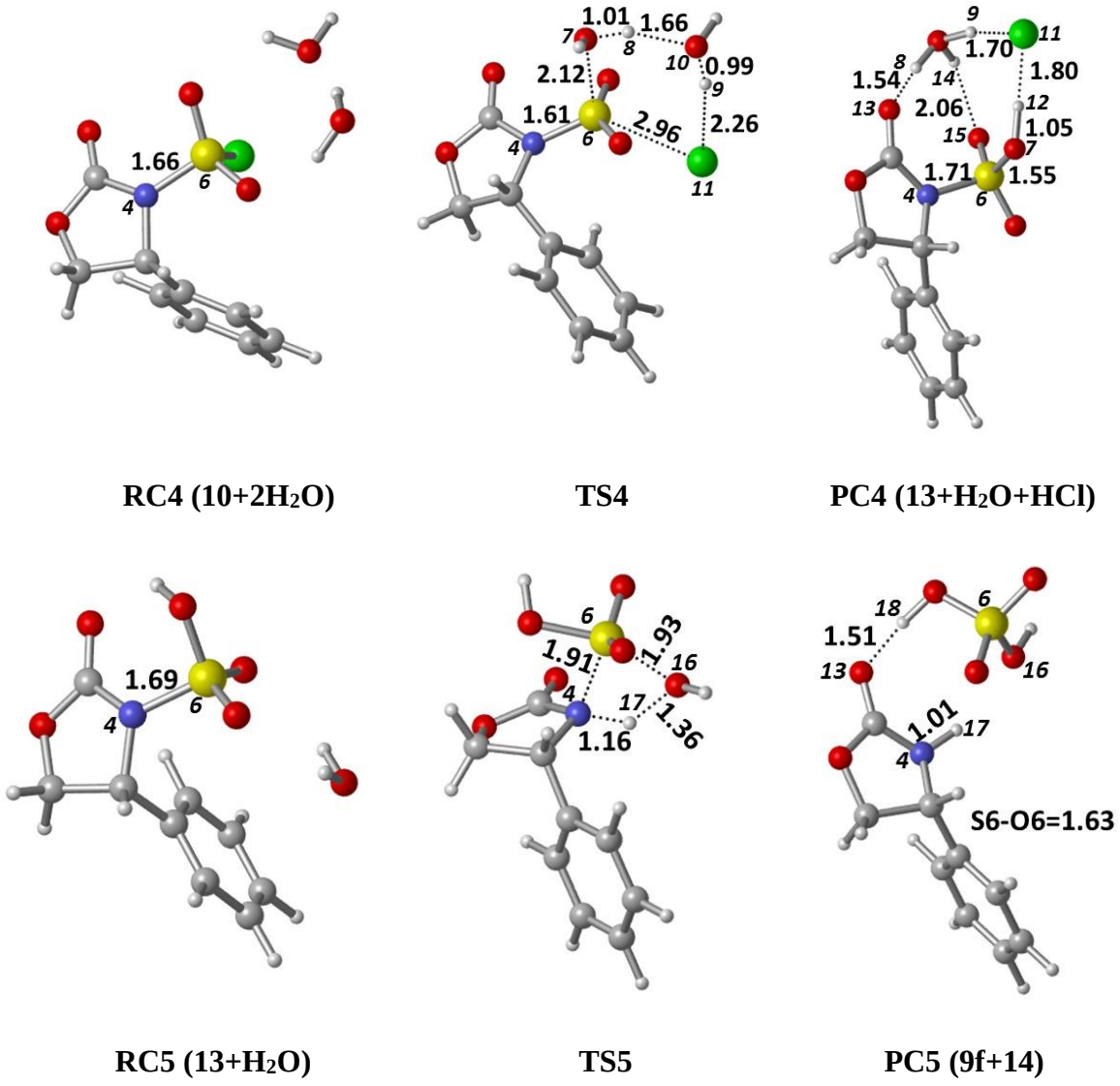

RC4 (10+2H₂O) **TS4** **PC4 (13+H₂O+HCl)**

RC5 (13+H₂O) **TS5** **PC5 (9f+14)**

Figure 8. Optimized geometries for the stationary points of path 2 at PCM(DCM)/M06-2X/6-31+G(d,p)//M06-2X/6-31+G(d,p) level. Distances are given in Å.

As it can be seen from the potential energy profile (Figure 5), water addition to **10** is likely to be rate-determining step for all reaction pathways. Comparison of the calculated Gibbs free energies of activation in DCM reveals that path 1b is the most plausible mechanism among the paths studied.

The reaction mechanism for the formation of five-membered cyclic carbonate **8f** has been also investigated theoretically and it is described below (Scheme 7).

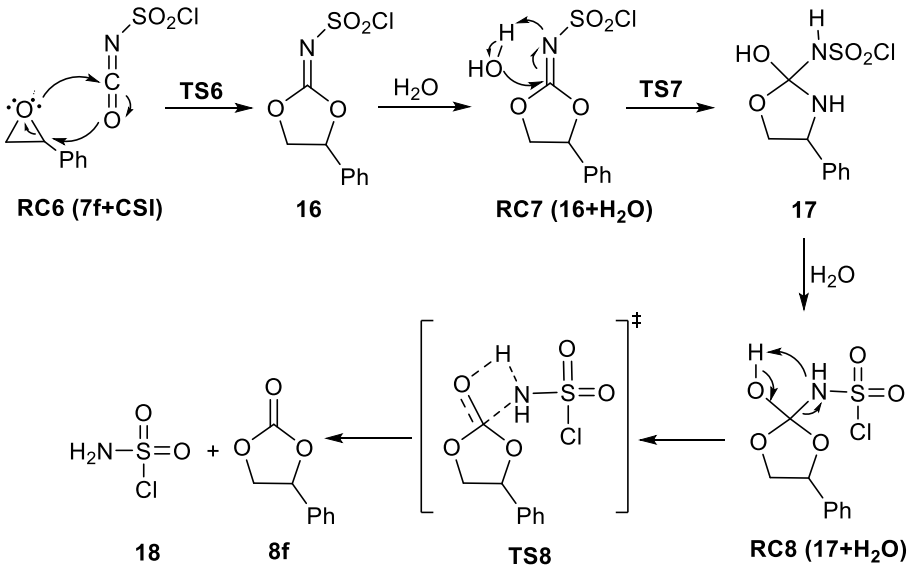

Scheme 7. Proposed mechanism for the formation of five-membered cyclic carbonate **8f**.

A similar transition state has been proposed for the formation of **8f** in the presence of CSI. The mechanism is thought to proceed by ring opening of the epoxide **7f** at the 2-position, followed by nucleophilic attack of O4 on C2 to afford **16**. The formation of **16** is exergonic by 30.4 kcal/ mol relative to **RC6 (7f+CSI)** (Figure 9). The optimized geometries are illustrated in Figure 10.

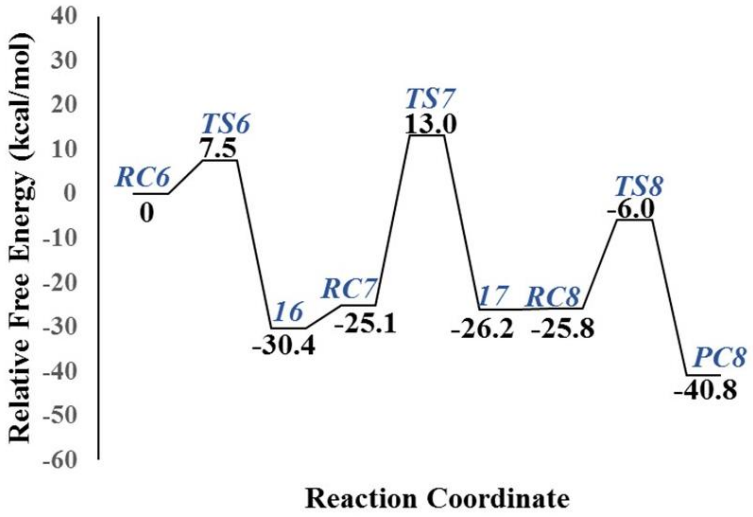

Figure 9. Potential energy profile and relative Gibbs free energies (kcal/mol) in DCM related to the formation of **8f** at PCM(DCM)/M06-2X/6-31+G(d,p)//M06-2X/6-31+G(d,p) level.

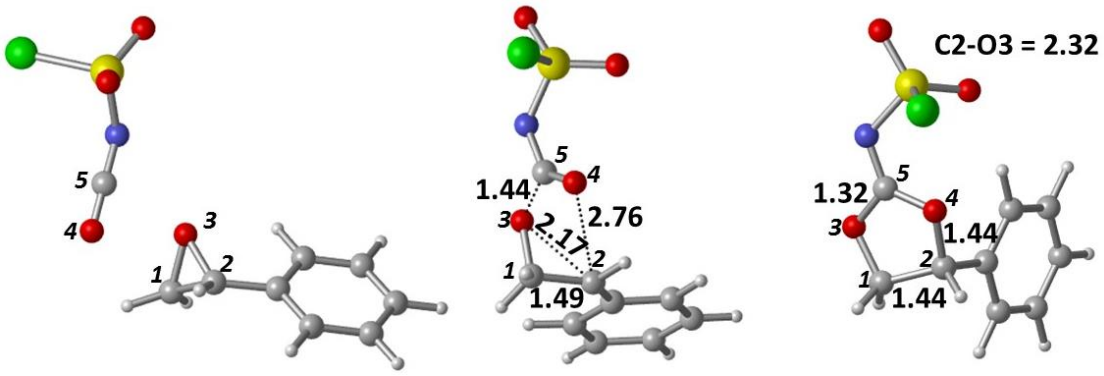

RC6 (7f+CSI) **TS6** **16**

Figure 10. Optimized geometries for the stationary points of step 1 for the formation of **16** at PCM(DCM)/M06-2X/6-31+G(d,p)//M06-2X/6-31+G(d,p) level. Distances are given in Å.

The intermediate **RC7 (16+H_2O)**, generated by the reaction of CSI with epoxide **7f**, reacts with a water molecule to yield **17**. Bond distance C5−N6 is predicted as 1.29, 1.41, and 1.46 Å in structures **RC7 (16+H_2O)**, **TS7**, and **17**, respectively (Figure 11). Besides, the C5−O7 distance is 1.58 Å in **TS7**; it is shortened to 1.39 Å in **17**. Here, while the O7−H8 single bond is broken, the N6−H8 bond is formed. The corresponding barrier was calculated to be 13.0 kcal/mol relative to initial reactant complex **RC6 (7f+CSI)** (Figure 9).

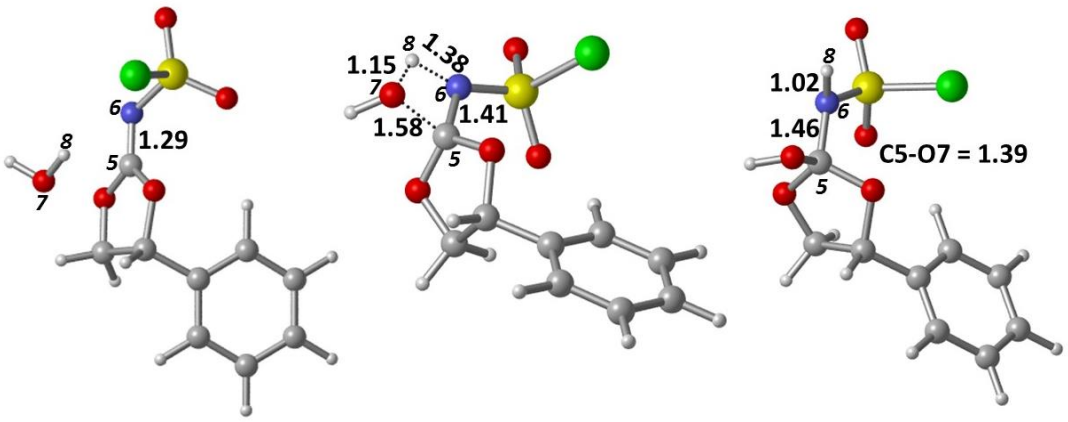

RC7 (16+H_2O) **TS7** **17**

Figure 11. Optimized geometries for the stationary points of step 2 for the formation of **17** at PCM(DCM)/M06-2X/6-31+G(d,p)//M06-2X/6-31+G(d,p) level. Distances are given in Å.

Elimination of **18**, accompanied by C=O bond formation, constitutes the final step of the reaction observed. Optimized structures are given in Figure 12. The elimination reaction, via

the transition state **TS8**, is facile and leads to stable product five-membered cyclic carbonate **8f**. (Figure 9).

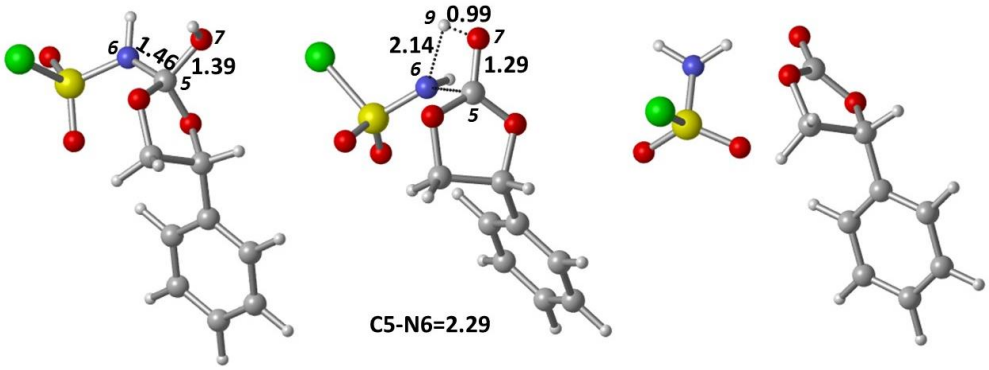

RC8 (17+H_2O) **TS8** **PC8 (8f+18)**

Figure 12. Optimized geometries for the stationary points of step 2 for the formation of **P8** at PCM(DCM)/M06-2X/6-31+G(d,p)//M06-2X/6-31+G(d,p) level. Distances are given in Å.

For the reaction of epoxides with CSI, Keshava Murthy and Dhar [41] suggested a stepwise reaction passing through a zwitterionic intermediate (Scheme 2a). De Meijere and coworkers [42] proposed a two-step process involving a 1,5-dipolar intermediate (Scheme 2b). However, in this work, we introduce a new mechanism by providing computational evidence for the asynchronous concerted pathway on the reaction of epoxides with CSI.

Conclusions

In summary, in the first part of the study, we have improved the general synthesis of five-membered cyclic carbonates and oxazolidinones from the various epoxides under mild conditions. This versatile conversion has enabled us to create a wide range of cyclic carbonates and oxazolidinones with a ratio close to (1:1) using a safe, inexpensive, metal-free reagent, simple purification method in shorter reaction times via one-pot reaction. We also described the synthesis of novel oxazolidinone derivatives **8i**, **8j** and 1,3-dioxolan-2-ones **9c** and **9i.** Moreover, an effective and simplistic procedure for the synthesis of **8a-h**, **9a-b**, **9d-h** and **9j** has been reported. The study presents a useful method for one-pot conversion of epoxides to protected 1,2-diols and 1,2-amino alcohols.

In the computational part of the study, the mechanisms leading to oxazolidinone **9f** and cyclic carbonate **8f** were examined. The calculated energy difference between the **TS1** (leading to **9f**)

and **TS6** (leading to **8f**) is very small (0.5 kcal/mol) but slightly in favor of carbonate **8f** which is in very good agreement with the experimental observation that isolated yields are 49% for **8f** and 42% for **9f**. The potential energy profiles of the formation of **8f** and **9f** are quite similar. IRC calculations revealed that first step of the mechanisms for the formation of **8f** and **9f** occur asynchronously although in a concerted fashion. The water addition steps are likely to be rate-determining for both reaction mechanisms. Besides, explicit inclusion of water molecules is crucial for lowering the energy barrier making the process plausible without changing the nature of the rate determining step of the formation of **9f**.

Methodology

All calculations have been carried with Gaussian 09 program package [57]. Geometry optimizations of all the minima and transition states involved have been performed using M06-2X [58,59] /6-31+G(d,p) level of theory. The M06-2X functional is known to show good performance in predicting the activation energies and transition state geometries of various reactions [58-60]. Harmonic vibrational frequencies have been calculated at the same level of theory for all stationary points to verify whether they are minima (no imaginary frequencies) or transition states (a single imaginary frequency). Thermodynamic calculations have been performed at 25 °C and 1 atm. The same level of intrinsic reaction coordinate (IRC) [61,62] calculations have been performed to check the energy profiles connecting each transition state to the two associated minima. The effect of the solvent environment on the reaction pathways has been taken into account by single-point energy calculations on the gas-phase stationary points using polarizable continuum model (PCM) [63] at M06-2X/6-31+G(d,p) level. Structural representations were generated using CYLView [64].

Experimental Section

General considerations: The epoxides were synthesized from related alkenes with m-CPBA. All solvents and reagents were used as purchased from commercial suppliers. Melting points were determined on a melting-point apparatus (Gallenkamp; WA11373) and are uncorrected. IR spectra were obtained from solutions in 0.1mm cells and in CH_2Cl_2 with a Perkin–Elmer spectrophotometer. ^{1}H and ^{13}C NMR spectra were recorded on an instruments (Varian and Bruker spectrometers) 400 and 100 MHz, respectively, and NMR shifts are presented as δ in ppm. Elemental analyses were performed on LECO CHNS-932 apparatus. MS spectra were

carried out on an LC/MS High-Resolution Time of Flight (TOF) Agilent 1200/6530 instrument. All column chromatography was performed on silica gel (60-mesh, Merck).

General procedure for the synthesis of five-membered cyclic carbonates and oxazolidinones:

Epoxide **7a** (500 mg, 4.54 mmol, 1 equiv) was dissolved in 20 mL dichloromethane. The reaction mixture was cooled to 0 °C, and chlorosulfonyl isocyanate (CSI, 707 mg, 4.99 mmol, 1.1 equiv) was added. Resulting solution was stirred at room temperature for 1 h. Then, the reaction mixture was added water (2 mL), and the mixture was stirred for 0.5 h. The reaction mixture was extracted with dichloromethane (3x20 mL). The organic phase was dried over sodium sulphate and concentrated. Purification was performed through column chromatography on silica gel eluting with hexane/EtOAc (4:1). In all reactions, 1,3-dioxolan-2-ones (**8a-j**) were isolated as the first fraction and oxazolidinones, (**9a-j)** as the second fraction.

Hexahydro-4,7-methanobenzo[d][1,3]dioxol-2-one (8a): [48] Colourless solid, (295 mg, yield 42%). ^{1}H NMR (400 MHz, $CDCl_3$, ppm) δ 4.51 (d, *J* = 1.46 Hz, 2H), 2.51-2.53 (m, 2H), 1.10-1.75 (m, 6H); ^{13}C NMR (100 MHz, $CDCl_3$, ppm) δ 155.9, 82.5, 40.4, 31.0, 23.0; IR ($CHCl_3$, cm^{-1}): 2969, 2879, 1802, 1784, 1372, 1164, 1068; Elemental Analysis Calcd for: C, 62.33; H, 6.54; found: 62.48; H, 6.42. HRMS (ESI) m/z calcd for $C_8H_{10}O_3$+: 154,0624; found [M+H]+ 154,0642.

Hexahydro-4,7-methanobenzo[d]oxazol-2(3H)-one (9a): [49] Colourless solid, (263 mg, yield 38%). ^{1}H NMR (400 MHz, $CDCl_3$, ppm) δ 4.80 (s, 1H), 3.92 (s, 2H), 2.68 (m, 2H). 1.93-0.83 (m, 6H); ^{13}C NMR (100 MHz, $CDCl_3$, ppm) δ 157.2, 86.5, 57.6, 40.4, 31.3, 22.5; IR ($CHCl_3$, cm^{-1}): 3366, 2961, 2930, 2885, 1801, 1781, 1709, 1644, 1351, 1182, 1067, 1001; Elemental Analysis Calcd for: C, 62.73; H, 7.24; N, 9.14; found: 62.64; H, 7.49; N, 9.32; HRMS (ESI) m/z calcd for $C_8H_{11}NO_2$+: 153,0784; found [M+H]+ 153,0765.

Hexahydro-4H-cyclohepta[d][1,3]dioxol-2-one (8b): [50] Colourless solid, (334 mg, yield 48%). ^{1}H NMR (400 MHz, $CDCl_3$, ppm) δ 4.82 (m, 2H), 1.94 (m, 4H), 1.80 (m, 2H), 1.63 (m, 1H), 1.50 (m, 1H), 1.32 (m, 2H); ^{13}C NMR (100 MHz, $CDCl_3$, ppm) δ 154.5, 79.6, 30.1, 29.7, 23.2; IR ($CHCl_3$, cm^{-1}): 2930, 2860, 1798, 1721, 1456, 1378, 1180, 1180, 1052; Elemental

Analysis Calcd for: C, 61.52; H, 7.74; found: 61.58; H, 7.52; HRMS (ESI) m/z calcd for $C_8H_{12}O_3$+: 156,0781; found [M+H]+ 156,0769.

Octahydro-2H-cyclohepta[d]oxazol-2-one (9b): [51] Colourless solid, (315 mg, yield 45%). ^{1}H NMR (400 MHz, $CDCl_3$, ppm) δ 4.86-4.92 (m, 1H), 4.59-4.36 (m, 1H), 2.32-1.21 (m, 10H), ^{13}C NMR (100 MHz, $CDCl_3$, ppm) δ 150.1, 79.2, 64.2, 30.3, 29.9, 28.5, 25.4, 22.7; IR ($CHCl_3$, cm^{-1}): 3250, 2931, 2859, 1803, 1748, 1414, 1369, 1176, 1087; Elemental Analysis Calcd for: C, 61.91; H, 8.44; N, 9.03; found: 61.73; H, 8.49; N, 9.34; HRMS (ESI) m/z calcd for $C_8H_{13}NO_2$+: 155,0941; found [M+H]+ 155,0964.

Octahydrocycloocta[d][1,3]dioxol-2-one (8c): [50] Colourless solid, (342 mg, yield 51%). ^{1}H NMR (400 MHz, $CDCl_3$, ppm) δ 4.72 (m, 2H), 1.99 (m, 4H), 1.73 (m, 2H), 1.48 (m, 4H), 1.25 (m, 2H); ^{13}C NMR (100 MHz, $CDCl_3$, ppm) δ 154.4, 81.4, 26.5, 26.2, 26.1; IR ($CHCl_3$, cm^{-1}): 2924, 1801, 1472, 1359, 1203, 1174, 1054; Elemental Analysis Calcd for: C, 63.51; H, 8.29; found: 63.42; H, 8.39; HRMS (ESI) m/z calcd for $C_9H_{14}O_3$+: 170,0937; found [M+H]+ 170,0956.

Octahydrocycloocta[d]oxazol-2(3H)-one (9c): Colourless solid, mp 91-93 ºC. (268 mg, yield 40%). ^{1}H NMR (400 MHz, $CDCl_3$, ppm) δ 4.70-4.65 (m, 1H), 4.57-4.53 (m, 1H), 2.28-0.95 (m, 12H). ^{13}C NMR (100 MHz, $CDCl_3$, ppm) δ 148.94, 80.71, 65.71, 26.94, 25.37, 28.41, 25.32, 24.93, 24.21; IR ($CHCl_3$, cm^{-1}): 3251, 2928, 2863, 1805, 1410, 1358, 1210, 1175, 1034; Elemental Analysis Calcd for: C, 63.88; H, 8.93; N, 8.28; found: 63.56; H, 9.04; N, 8.54; HRMS (ESI) m/z calcd for $C_9H_{15}NO_2$+: 169,1097; found [M+H]+ 169,1086.

Trans 4,5-diphenyl-1,3-dioxolan-2-one (8d): [50] Colourless solid, (263 mg, yield 43%). ^{1}H NMR (400 MHz, $CDCl_3$, ppm) δ 5.42 (s, 2H), 7.31-7.33 (m, 3H), 7.43-7.45 (m, 6H). ^{13}C NMR (100 MHz, $CDCl_3$, ppm) δ 154.3, 135.1, 130.0, 129.5, 126.3, 85.6; IR ($CHCl_3$, cm^{-1}): 3064, 2925, 1808, 1457, 1257, 1167, 1044; Elemental Analysis Calcd for: C, 74.99; H, 5.03; found: C, 75.32; H, 5.21; HRMS (ESI) m/z calcd for $C_{15}H_{12}O_3$+: 240,0781; found [M+H]+ 240,0796.

Trans 4,5-diphenyloxazolidin-2-one (9d): [52] Colourless solid, (208 mg, yield 34%). ^{1}H NMR (400 MHz, $CDCl_3$, ppm) δ 7.39-7.42 (m, 6H) 7.25-7.32 (m, 4H), 5.48 (bs, 1H), 5.30 (m, 1H), 4.75 (d, J = 7.7 Hz, 1H); ^{13}C NMR (100 MHz, $CDCl_3$, ppm) δ 158.7, 138.5, 137.5, 129.5, 129.3, 129.2, 128.5, 126.7, 126.1, 86.4, 65.1; IR ($CHCl_3$, cm^{-1}): 3290, 2923, 2853, 1754, 1456, 1380, 1199, 1015; Elemental Analysis Calcd for: C, 75.30; H, 5.48; N, 5.85; found: C, 75.42; H, 5.36; N, 5.67; HRMS (ESI) m/z calcd for $C_{15}H_{13}NO_2$+; 239,0941; found [M+H]+ 239,0947.

Cis 4,5-diphenyl-1,3-dioxolan-2-one (8e): [50] Colourless solid, (269 mg, yield 44%). ^{1}H NMR (400 MHz, $CDCl_3$, ppm) δ 7.42-7.45 (m, 6H). 7.30-7.33 (m, 4H). 5.44 (s, 2H); ^{13}C NMR (100 MHz, $CDCl_3$, ppm) δ 154.3, 135.0, 130.0, 127.3, 126.3, 85.6; IR ($CHCl_3$, cm^{-1}): 2918, 1811, 1454, 1275, 1091; Elemental Analysis Calcd for: C, 74.99; H, 5.03; found: C, 75.12; H, 5.24; HRMS (ESI) m/z calcd for $C_{15}H_{12}O_3$+: 240,0781; found [M+H]+ 240,0794.

Cis 4,5-diphenyloxazolidin-2-one (9e): [52] Colourless solid, (250 mg, yield 41%). ^{1}H NMR (400 MHz, $CDCl_3$, ppm) δ 7.12-7.09 (m, 6H), 6.98-6.94 (m, 4H), 5.95 (d, *J* = 8.1 Hz, 1H), 5.5 (bs, 1H), 5.2 (d, *J* = 8.1 Hz, 1H); ^{13}C NMR (100 MHz, $CDCl_3$, ppm) δ 160.1, 136.2, 128.6, 128.5, 128.3, 128.1, 127.2, 126.7, 126.3, 126.0, 82.6, 61.6; IR ($CHCl_3$, cm^{-1}): 3295, 2923, 1754, 1455, 1356, 1217, 1091, 1020; Elemental Analysis Calcd for: C, 75.30; H, 5.48; N, 5.85; found: C, 75.36; H, 5.57; N, 5.66; HRMS (ESI) m/z calcd for $C_{15}H_{13}NO_2$+: 239,0941; found [M+H]+ 239,0955.

4-Phenyl-1,3-dioxolan-2-one (8f): [16] White solid, (355 mg, yield 49%). ^{1}H NMR (400 MHz, $CDCl_3$, ppm) δ 7.27-7.46 (m, 5H), 5.68 (t, *J* = 8.6 Hz, 1H), 4.82 (t, *J* = 8.6 Hz, 1H), 4.36 (t, *J* = 8.6 Hz, 1H); ^{13}C NMR (100 MHz, $CDCl_3$, ppm) δ 155.0, 136.0, 129.5, 129.2, 126.0, 78.2, 71.4; IR ($CHCl_3$, cm^{-1}): 2932, 1809, 1795, 1457, 1358, 1270, 1168, 1067; Elemental Analysis Calcd for: C, 65.85; H, 4.91; found: C, 65.92; H, 4.85; HRMS (ESI) m/z calcd for $C_9H_8O_3$+: 164,0468; found [M+H]+ 164,0475.

4-Phenyloxazolidin-2-one (9f): [16] White solid, (285 mg, yield 42%). ^{1}H NMR (400 MHz, $CDCl_3$, ppm) δ 7.38-7.43 (m, 5H), 5.46 (s, 1H, NH), 4.98 (dd, *J* = 8.6, 7.0 Hz, 1H), 4.76 (dd, *J* = 8.6, 7.0 Hz, 1H), 4.21 (dd, *J* = 8.6, 7.0 Hz, 1H); ^{13}C NMR (100 MHz, $CDCl_3$, ppm) δ 56.6, 72.8, 126.3, 129.2, 129.5, 139.6. 158.2; IR ($CHCl_3$, cm^{-1}): 3284, 2922, 1744, 1457, 1404, 1238, 1040; Elemental Analysis Calcd for: C, 66.25; H, 5.56; N, 8.58; found: C, 66.48; H, 5.32; N, 8.45; HRMS (ESI) m/z calcd for $C_9H_9NO_2$+: 163,0628; found [M+H]+ 163,0643.

4-Benzyl-1,3-dioxolan-2-one (8g): [16] Colourless oil, (270 mg, yield 41%). ^{1}H NMR (400 MHz, $CDCl_3$, ppm) δ 2.99 (dd, *J* = 6.7, 14.2 Hz, 1H), 3.15 (dd, *J* = 6.4, 14.2 Hz, 1H), 4.17 (dd, *J* = 6.9, 8.6 Hz, 1H), 4.44 (t, *J* = 8.1 Hz, 1H), 4.93 (m, 1H), 7.18-7.25 (m, 2H), 7.28-7.36 (m, 3H); ^{13}C NMR (100 MHz, $CDCl_3$, ppm) δ 155.1, 134.1, 129.6, 129.2, 127.8, 77.1, 68.7, 39.8; IR ($CHCl_3$, cm^{-1}): 2921, 1803, 1455, 1371, 1272, 1170, 1080; Elemental Analysis Calcd for: C, 67.41; H, 5.66; found: C, 67.49; H, 5.72; HRMS (ESI) m/z calcd for $C_{10}H_{10}O_3$+: 178,0624; found [M+H]+ 178,0643.

4-Benzyloxazolidin-2-one (9g): [53] Colourless solid, (230 mg, yield 35%). ^{1}H NMR (400 MHz, $CDCl_3$, ppm) δ 7.17-7.35 (m, 5H), 4.84 (bs, 1H), 4.47- 4.49 (m, 1H), 4.07-4.13 (m, 2H), 2.76-2.84 (m, 2H), ^{13}C NMR (100 MHz, $CDCl_3$, ppm) δ 159.6, 135.8, 129.1, 128.9, 127.3, 69.6, 53.7, 41.4; IR ($CHCl_3$, cm^{-1}): 3282, 2925, 1744, 1456, 1410, 1223, 1030; Elemental Analysis Calcd for: C, 67.78; H, 6.26; N, 7.90 found: C, 67.71; H, 6.38; N, 7.75; HRMS (ESI) m/z calcd for $C_{10}H_{11}NO_2$+: 177,0784; found [M+H]+ 177,0789.

8,8a-dihydro-3aH-indeno[1,2-d][1,3]dioxol-2-one (8h): [54] White solid, (300 mg, yield 45%). ^{1}H NMR (400 MHz, $CDCl_3$, ppm) δ 7.32-7.53 (m, 4H), 6.01 (d, J = 6.8 Hz, 1H), 5.44-5.46 (m, 1H), 3.40 (m, 2H); ^{13}C NMR (100 MHz, $CDCl_3$, ppm) δ 154.9, 140.3, 136.7, 131.3, 128.5, 126.8, 125.6, 83.7, 79.7, 38.3; IR ($CHCl_3$, cm^{-1}): 2925, 1789, 1463, 1362, 1160, 1058, 1016; Elemental Analysis Calcd for: C, 68.18; H, 4.58; found: C, 68.34; H, 4.65; HRMS (ESI) m/z calcd for $C_{10}H_8O_3$+: 176,0468; found [M+H]+ 176,0478.

3,3a,8,8a-tetrahydro-2H-indeno[1,2-d]oxazol-2-one (9h): [52] White solid, (265 mg, yield 40%). ^{1}H NMR (400 MHz, $CDCl_3$, ppm) δ 7.25 –7.36 (m, 4H), 7.10 (bs, 1H), 5.40–5.45 (m, 1H), 5.19 (d, *J* = 7.1 Hz, 1H), 3.42 (d, *J* = 18.5 Hz 1H), 3.34 (d, *J* = 16.9 Hz, 1H); ^{13}C NMR (100 MHz, $CDCl_3$, ppm) δ 159.7, 140.2, 139.6, 129.4, 127.7, 125.4, 124.9, 80.7, 61.3, 38.9; IR ($CHCl_3$, cm^{-1}): 3490, 2921, 1803, 1455, 1272, 1170, 1161; Elemental Analysis Calcd for: C, 68.56; H, 5.18; N, 8.00; found: C, 68.64; H, 5.34; N, 8.23; HRMS (ESI) m/z calcd for $C_{10}H_9NO_2$+: 175,0628; found [M+H]+ 175,0643.

3a,4,9,9a-tetrahydro-4,9-methanonaphtho[2,3-d][1,3]dioxol-2-one (8i): Colourless solid, mp 102-104 ºC. (287 mg, yield 43%). ^{1}H NMR (400 MHz, $CDCl_3$, ppm) δ 7.18-7.27 (m, 4H), 4.62 (s, 2H), 3.62 (s, 2H), 2.16 (s, 2H); ^{13}C NMR (100 MHz, $CDCl_3$, ppm) δ 154.0, 142.2, 128.1, 123.3, 80.5, 47.9, 41.6; IR ($CHCl_3$, cm^{-1}): 2932, 1804, 1460, 1160, 1066, 976; Elemental Analysis Calcd for: C, 71.28; H, 4.98; found: C, 71.43; H, 4.73; HRMS (ESI) m/z calcd for $C_{12}H_{10}O_3$+: 202,0624; found [M+H]+ 202,0637.

3a,4,9,9a-tetrahydro-4,9-methanonaphtho[2,3-d]oxazol-2(3H)-one (9i): Colourless solid, mp 133-135 ºC. (235 mg, yield 37%). ^{1}H NMR (400 MHz, $CDCl_3$, ppm) δ 7.20-7.30 (m, 4H). 4.94 (s, 2H), 3.95 (s, 2H), 2.24-2.27 (m, 1H), 2.11-2.17 (m, 1H); ^{13}C NMR (100 MHz, $CDCl_3$, ppm) δ 162.7, 141.4, 128.5, 123.6, 85.1, 57.8, 47.9, 41.9, 29.9; IR ($CHCl_3$, cm^{-1}): 3340, 2918, 1802, 1647, 1461, 1368, 1166, 1001; Elemental Analysis Calcd for: C, 71.63; H, 5.51; N, 6.96;

found: C, 71.48; H, 5.72; N, 6.79; HRMS (ESI) m/z calcd for $C_{12}H_{11}NO_2$+: 201,0784; found [M+H]+ 201,0796.

3a-Phenylhexahydrobenzo[d][1,3]dioxol-2-one (8j): Colourless solid, mp 97-99 ^{o}C. (275 mg, yield 44%). ^{1}H NMR (400 MHz, $CsDCl_3$, ppm) δ 7.27-7.42 (m, 5H), 4.81 (t, *J* = 4.4 Hz, 1H), 2.09-2.18 (m, 8H); ^{13}C NMR (100 MHz, $CDCl_3$, ppm) δ 154.7. 140.9, 129.1, 128.8, 124.9, 85.2, 81.2, 34.9, 26.7, 19.7, 18.2; IR ($CHCl_3$, cm^{-1}): 2935, 2865, 1803, 1449, 1205, 1028; Elemental Analysis Calcd for: C, 71.54; H, 6.47; found: C, 71.65; H, 6.38; HRMS (ESI) m/z calcd for $C_{13}H_{14}O_3$+: 218,0937; found [M+H]+ 218,0946.

3a-Phenylhexahydrobenzo[d]oxazol-2(3H)-one (9j): [55] Colourless oil, (265 mg, yield 42%). ^{1}H NMR (400 MHz, $CDCl_3$, ppm) δ 7.42–7.38 (m, 2H), 7.36–7.33 (m, 2H), 7.30–7.26 (m, 1H), 4.66 (t, *J* = 4.2 Hz, 1H), 2.19–2.14 (m, 1H), 2.06–2.01 (m, 1H), 1.89–1.66 (m, 4H), 1.62–1.53 (m, 2H); ^{13}C-NMR (100 MHz, $CDCl_3$, ppm) δ 159.8, 143.3, 128.6, 127.8, 125.3, 82.0, 61.8, 34.8, 25.9, 19.5, 17.6; IR ($CHCl_3$, cm^{-1}): 3220, 2943, 1803, 1448, 1205, 1028, 1005; Elemental Analysis Calcd for: C, 71.87; H, 6.96; N, 6.45; found: C, 71.68; H, 6.91; N, 6.54; HRMS (ESI) m/z calcd for $C_{13}H_{15}NO_2$+: 217,1097; found [M+H]+ 217,1086.

Acknowledgements

We are grateful to the Scientific Research Project of Atatürk University of Turkey (BAP) for a grant [2016/158].

References

[1] Stevens, D. L.; Dotter, B.; Madaras-Kelly, K. *Expert Rev. Anti. Infect. Ther.* **2004**, *2*, 51–59.

[2] Wang, J.; Xia, L.; Wang, R.; Cai, Y. *Front. Pharmacol.* **2019**, *10*, 1–10.

[3] Barbachyn, M. R.; Ford, C. W. *Angew. Chemie - Int. Ed.* **2003**, *42*, 2010–2023.

[4] Orac, C. M.; Zhou, S.; Means, J. A.; Boehm, D.; Bergmeier, S. C.; Hines, J. V. *J. Med. Chem.* **2011**, *54*, 6786–6795.

[5] Ager, D. J.; Prakash, I.; Schaad, D. R. *Chem. Rev.* **1996**, *96*, 835–875.

[6] Flynn, B. L.; Manchala, N.; Krenske, E. H. *J. Am. Chem. Soc.* **2013**, *135*, 9156-9163.

[7] Wan, N.; Zhou, X.; Ma, R.; Tian, J.; Wang, H.; Cui, B.; Han, W.; Chen, Y. *Adv. Synth. Catal.* **2020**, *362* (5), 1201–1207.

[8] Narina, S. V.; Kumar, T. S.; George, S.; Sudalai, *Tetrahedron Lett.* **2007**, *48*, 65–68.

[9] Asano, M.; Nagasawa, C.; Suzuki, M.; Nishiyama, S.; Sugai, T. *Biosci. Biotechnol. Biochem.* **2005**, *69*, 145–148.

[10] Xin, Q.; Fan, H.; Guo, B.; He, H.; Gao, S.; Wang, H.; Huang, Y.; Yang, Y. *J. Med. Chem.* **2011**, *54*, 7493–7502.

[11] Zhanel, G. G.; Love, R.; Adam, H.; Golden, A.; Zelenitsky, S.; Schweizer, F.; Gorityala, B.; Lagacé-Wiens, P. R. S.; Rubinstein, E. Walkty, A. *Drugs* **2015**, *75*, 253–270.

[12] Mai, A.; Artico, M.; Esposito, M.; Ragno, R.; Sbardella, G.; Massa, S. *Il Farmaco* **2003**, *58*, 231–241.

[13] Youdim, M. B. H.; Edmondson, D.; Tipton, K. F. *Nat. Rev. Neurosci.* **2006**, *7*, 295-309.

[14] Gunal, S. E.; Tuncel, S. T.; Kelekci, N. G.; Ucar, G.; Dursun, B. Y.; Erdem, S. S.; Dogan, I. *Bioorg. Chem.* **2018**, *77*, 608–618.

[15] Clements, J. H. *Ind. Eng. Chem. Res.* **2003**, *42*, 663–674.

[16] Peña-López, M.; Neumann, H.; Beller, M. *European J. Org. Chem.* **2016**, *2016*, 3721-3727.

[17] Comerford, J. W.; Ingram, I. D. V; North, M.; Wu, X. *Green Chemistry* **2015**, *17*, 1966–1987.

[18] Aravindan, V.; Gnanaraj, J.; Madhavi, S.; Liu, H. K. *Chem. - A Eur. J.* **2011**, *17*, 14326–14346.

[19] Tezuka, K.; Koda, K.; Katagiri, H.; Haba, O. *Polym. Bull.* **2015**, *72*, 615–626.

[20] Azechi, M.; Matsumoto, K.; Endo, T. *J. Polym. Sci. Part A Polym. Chem.* **2013**, *51*, 1651–1655.

[21] Brandão, P.; Pineiro, M.; Pinho e Melo, T. M. V. D. *European J. Org. Chem.* **2019**, *2019*, 7188–7217.

[22] Matsunaga, S.; Kumagai, N.; Harada, S.; Shibasaki, M. *J. Am. Chem. Soc.* **2003**, *125*,4712–4713.

[23] Tominaga, K. I.; Sasaki, Y. *Synlett* **2002**, *2*, 307–309.

[24] R Morales-Nava, R.; Fernández-Zertuche, M.; Ordóñez, M. *Molecules* **2011**, *16*, 8803–8814.

[25] Pulla, S.; Unnikrishnan, V.; Ramidi, P.; Sullivan, S. Z.; Ghosh, A.; Dallas, J. L.; Munshi, P. *Journal Mol. Catal. A, Chem.* **2011**, *338*, 33–43.

[26] Liu, J.; Peng, X.; Liu, J.; Zheng, S. *Tetrahedron letters*. **2007**, *48*, 929–932.

[27] Gabriele, B.; Salerno, G.; Brindisi, D.; Costa, M.; Paolo Chiusoli, G. *Org. Lett.* **2000**, *2*, 625-627.

[28] Zhou, M.; Zheng, X.; Wang, Y.; Yuan, D.; Yao, Y. *ChemCatChem*. **2019**, *11*, 5783–5787.

[29] Feroci, M.; Orsini, M.; Sotgiu, G.; Rossi, L.; Inesi, A. *J. Org. Chem.* **2005**, *70*, 7795–7798.

[30] Miller, A. W.; Nguyen, S. B. T. *Org. Lett.* **2004**, *6*, 2301–2304.

[31] Speranza, G. P.; Peppel, W. J. *J. Org. Chem.* **1958**, *23*, 1922–1924.

[32] Baronsky, T.; Beattie, C.; Harrington, R. W.; Irfan, R.; North, M.; Osende, J. G.; Young, C. *ACS Catal.* **2013**, *3*, 790–797.

[33] North, M.; Pasquale, R.; Young, C.; North, M. *Green Chemistry* **2010**, *12*, 1514–1539.

[34] Aoyagi, N.; Furusho, Y.; Endo, T. *Synthesis (Stuttg).* **2020**, *52*, 150–158.

[35] Martín, C.; Fiorani, G.; Kleij, A. W. *ACS Catal.* **2015**, *5*, 1353–1370.

[36] Shimojo, M.; Matsumoto, K.; Hatanaka, M. *Tetrahedron* **2000**, *56*, 9281–9288.

[37] Shellhamer, D. F.; Davenport, K. J.; Hassler, D. M.; Hickle, K. R.; Thorpe, J. J.; Vandenbroek, D. J.; Heasley, V. L.; Boatz, J. A.; Reingold, A. L.; Moore, C. E. *J.Org. Chem.* **2010**, *75*, 7913–7916

[38] Shellhamer, D. F.; Alexander, K. L.; Bunting, S. A.; Elwin, S. L.; Licata, C. J.; Milligan, J. C.; Robinson, R. D.; Shipowick, D. E.; Smith, L. B.; Perry, M. C. *Synth.* **2015**, *47*, 1944–1950

[39] Dhar, D. N.; Kesheva Murthy, K. S. *Synthesis* **1986**, *6*, 437–449.

[40] Murthy, K. S. K.; Dhar, D. N. *Synth. Commun.* **1984**, *14*, 687–695

[41] Murthy, K. S. K.; Dhar, D. N. *J. Heterocycl. Chem.* **1984**, *21*, 1721–1725.

[42] Lorincz, T.; Erden, I.; Näder, R.; de Meijere, A. *Synth. Commun.* **1986**, *16*, 123–130.

[43] Atmaca, U.; Yıldırım, A.; Taslimi, P.; Çelik, S. T.; Gülçin, İ.; Supuran, C. T.; Çelik, M. *J. Biochem. Mol. Toxicol.* **2018**, *32*, e22173

[44] Daryadel, S.; Atmaca, U.; Taslimi, P.; Gülçin, İ.; Çelik, M. *Arch. Pharm. (Weinheim).* **2018**, *351*, e1800209

[45] Atmaca, U.; Daryadel, S.; Taslimi, P.; Çelik, M.; Gülçin, İ. *Arch. Pharm. (Weinheim).* **2019**, *352*, e1900200

[46] Atmaca, U. *Tetrahedron* **2019**, *75* (34), 130467.

[47] Daruì, A.; Roca-López, D.; Tejero, T.; Merino, P. *J. Org. Chem.* **2016**, *81*, 673–680.

[48] Laserna, V.; Fiorani, G.; Whiteoak, C. J.; Martin, E.; Escudero-Adán, E.; Kleij, A. W. *Angew. Chemie - Int. Ed.* **2014**, *53*, 10416-10419.

[49] Scholz, K.H.; Heine, H. G.; Hartmann, W. *Liebigs Ann. Chem.* **1977**, *11*, 2027-2035.

[50] Steinbauer, J.; Spannenberg, A.; Werner, T. *Green Chem.* **2017**, *19*, 3769-3779.

[51] Hu, N. X.; Aso, Y.; Otsubo, T.; Ogura, F. *J. Org. Chem.* **1989**, *54*, 4398-4404.

[52] Yang, X.; Bumbu, V. D.; Liu, P.; Li, X.; Jiang, H.; Uffman, E. W.; Guo, L.; Zhang, W.; Jiang, X.; Houk, K. N. *J. Am. Chem. Soc.* **2012**, *134*, 17605-17612.

[53] Sukhanova, A. A.; Puchkin, I. A.; Vasil'ev, A. A.; Zlotin, S. G. *Tetrahedron Asymmetry* **2017**, 28, 1834-1841.

[54] Miceli, C.; Rintjema, J.; Martin, E.; Escudero-Adán, E. C.; Zonta, C.; Licini, G.; Kleij, A. W. *ACS Catal.* **2017**, 7, 2367-2373.

[55] Lebel, H.; Mamani Laparra, L.; Khalifa, M.; Trudel, C.; Audubert, C.; Szponarski, M.; Dicaire Leduc, C.; Azek, E.; Ernzerhof, M. *Org. Biomol. Chem.* **2017**, 15, 4144-4158.

[56] Tantillo, D. J. *J. Phys. Org. Chem.* **2008**, *21*, 561–570.

[57] Frisch M. J., Trucks G. W., Schlegel H. B. Gaussian 09, Revision B.01. (Wallingford CT: Gaussian, Inc. **2009**). (For the full citation see SI)

[58] Zhao, Y.; Truhlar, D. G. *Theor Chem Acc*. **2008**, *120*, 215–241

[59] Zhao, Y.; Truhlar, D. G. *Acc Chem Res*. **2008**, *4*, 157–167.

[60] Guleli, M.; Erdem, S. S.; Ocal, N.; Erden, I.; Sari, O. *Res. Chem. Intermed.* **2019**, *45*, 2119–2134.

[61] Gonzalez, C.; Schlegel, H. B. *J Chem Phys*. **1989**, *90*, 2154–2161

[62] Gonzalez, C.; Schlegel, H. B. *J Phys Chem*. **1990**, *94*, 5523–5527.

[63] Miertus, S.; Scrocco, E.; Tomasi, J. *Chem. Phys*. **1981**, *55*, 117–129.

[64] Legault, C. Y. *CYLview*, 1.0b; Université de Sherbrooke: Sherbrooke, Québec, Canada, **2009**. http://www.cylview.org.